DOI: 10.61782/fa.2025.0627

FORUM ACUSTICUM EURONOISE 2025

NUMERICAL AND EXPERIMENTAL ZIG-ZAG TRIP EFFECTS ON A LOW REYNOLDS NUMBER PROPELLER

Lattari Mateus Grassano[1*] **Beck Augusto**[1*] **Vicente Gabriel Caldeira**[1]
Silva Filipe Dutra[2] **Salazar Juan Pablo Lima Costa**[2]
Cordioli Júlio Apolinário[1] **Deschamps César José**[1]
[1] Federal University of Santa Catarina, Department of Mechanical Engineering, Florianópolis, Brazil
[2] Federal University of Santa Catarina, Department of Mobility Engineering, Joinville, Brazil

ABSTRACT

Hybrid RANS/LES simulations have emerged as effective computational aeroacoustics tools for propeller noise, combining benefits of modeled and scaled turbulence, i.e., RANS and LES, respectively. The latter is chosen for solving tip vortices, turbulent wakes, vortex shedding, and blade-vortex interactions. The former is suitable for boundary layers modeled by wall functions, ensuring a feasible computational cost, but demanding the prescription of boundary layer regimes and its transition line. However, a key challenge lies in triggering LES models, as a physical obstacle on the transition is often required, such as zig-zag protuberant tripping on the span transition. Although tripping is a numerical strategy, the impact of the structure on a real propeller needs clarification. This work aims to numerically and experimentally investigate various propeller tripping span locations, both arbitrarily chosen and determined using low-order viscous panel transition models. Numerical simulations with PowerFLOW Lattice Boltzmann model are compared with tripped propeller measurements. Our results show that simulations differed from experimental broadband noise by 10-15 dB, depending on where the tripping is placed. Thrust and torque highlight a 15tripped propeller yielded consistent results, but turbulent variables analysis reveals the importance of the tripping for triggering LES

*__Corresponding author__: mateus.grassano@polo.ufsc.br.

Keywords: *hybrid RANS/LES, BLT Devices, propeller tripping, aeroacoustics, lattice boltzmann method).*

1. INTRODUCTION

Aerodynamic performance at low Reynolds numbers, typically encountered by small unmanned aerial vehicles (UAVs), micro air vehicles, and sections of wind turbine blades, is often significantly affected by complex boundary layer phenomena. A key challenge in this regime is the formation of Laminar Separation Bubbles (LSBs), regions where the laminar boundary layer separates, transitions to turbulence, and potentially reattaches. These LSBs can lead to increased drag, reduced lift, and unsteady aerodynamic loads, thereby degrading overall efficiency and performance. Consequently, considerable research effort has been directed towards understanding and mitigating these effects, often through the application of boundary layer tripping (BLT) devices designed to force transition from laminar to turbulent flow upstream of the natural separation point or to enhance numerical models to better predict the transition process.

For airfoils, Reference [1] demonstrated experimentally that relatively thin 2D trips could significantly alter drag characteristics on airfoils featuring large LSBs. However, these devices did not consistently enhance performance compared to airfoils without trips having smaller separation bubbles. Complementing this, numerical simulations indicated substantial reductions in drag (up to 15.48%) for the E216 airfoil using optimized BLTs, provided the device height remained modest [2]. Additionally, trip height and spanwise homogeneity influence noise generation on a NACA-0012 airfoil, concluding that

broadband noise sensitivity primarily depended on trip height due to its effect on boundary layer thickness and velocity fluctuations perpendicular to the surface [3].

Regarding low-Reynolds-number propellers, PowerFLOW [4] numerical simulations using BLT deviced for correcting the transition point and physics of the flow emphasized the necessity of accurately capturing laminar-turbulent transition phenomena to correctly predict both aerodynamic performance and noise. A combined experimental and numerical approach revealed that zig-zag BLT could enhance the simulations fidelity to experiments while generating negligible spurious noise sources [5]. This was latter expanded in subsequent works [6] finding generally marginal sensitivity of thrust and torque to the position of transition devices. However, broadband noise was slightly more affected, particularly at higher advance ratios, indicating that careful selection of tripping device location is important.

Lastly, additional references [7, 8] specifically addressed broadband noise reduction in low-Reynolds-number drone propellers, correlating noise sources with laminar separation bubbles on blade suction surfaces. Introducing leading-edge trips effectively eliminated these bubbles at low angles of attack, significantly reducing broadband noise without compromising propeller efficiency. Experimental results from static and wind-tunnel tests showed noise reductions between 4 dB(A) and 5 dB(A), demonstrating the practical benefits of forced transition.

Bearing in mind the importance of LSBs and the potential of tripping devices for performance and noise mitigation, this work aims to numerically and experimentally investigate the aerodynamic and noise levels of various propeller tripping span locations, both arbitrarily chosen and determined using low-order viscous panel transition models, obtaining a calculated natural transition line. The research employs experimental and hybrid computational approach, combining Reynolds-Averaged Navier-Stokes (RANS) simulations with a Lattice Boltzmann Method (LBM) for aeroacoustic predictions, relying on the existant model in PowerFLOW, to provide insights into the complex interactions between flow structures, trips, and noise generation mechanisms. After this points this paper is divided into a methodology and a section dedicated to the results.

2. METHODOLOGY

2.1 Theoretical Methodology

In this study, the hybrid RANS/LES LBM-based model chosen for the numerical results relies on PowerFLOW [4]. Instead of using the traditional Navier-Stokes equations that view fluid as a continuous substance, LBM works from a particle perspective, based on kinetic theory. It simplifies the problem by not tracking every individual particle, but rather by describing the statistical behavior of particle groups using a probability distribution function. This function unveils the probability of finding particles with certain velocities at specific points in space and time. The evolution of this distribution is governed by the Boltzmann equation, which includes terms for particle movement and collisions. PowerFLOW uses a simplified collision model (BGK), which makes the LBM computationally efficient and well-suited for complex simulations on powerful computers. Within PowerFLOW, the LBM is implemented on a Cartesian volumetric grid of cubic elements called "Voxels" for the fluid space. From the solved particle distributions, the software calculates macroscopic flow properties like fluid density and velocity, although it assumes the temperature remains constant. This hybrid approach directly calculates the large-scale turbulent eddies while using a turbulence model (RNG k-ϵ) to represent the effects of subgrid scales, allowing for detailed and accurate simulation of complex fluid flow and noise phenomena [4].

2.2 Experimental description

This study investigated five different configurations related to boundary layer tripping on a propeller: one baseline case without a BLT device (tripping), three cases triped 0.25, 0.50, and 0.75 of the local blade chord (C) respectively, and a final case where tripping was applied at a position automatically determined by a Blade Element Momentum Theory code as the likely natural transition location, using a method similar to reference ([5]). All experiments were performed under static conditions, meaning zero freestream velocity (advance ratio J=0), with the propeller rotating at 5000 rpm.

The experiments were conducted in a semi-anechoic chamber using a dedicated test rig, replicating the simulated conditions including the different tripping positions. Key measurements included propeller rotational speed via a shaft encoder, aerodynamic forces and moments using a 6-axis load cell, and acoustic pressure fluctuations cap-

tured by an array of 9 microphones placed 2 meters from the propeller (Figure 1) in angles ranging from -45 to 45 along the propeller downstream to its upstream. Significant efforts were made to minimize experimental noise and interference, including the use of acoustic absorption materials, vibration damping, aerodynamic fairings, and flow-straightening screens.

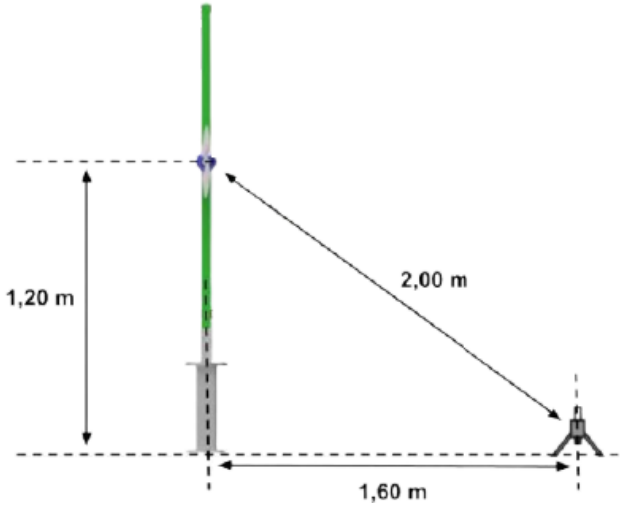

Figure 1: Microphone array setup.

Due to manufacturing challenges, the complex parametric zig-zag tripping geometry used in simulations was approximated experimentally using straight strips of thin (0.20 mm) adhesive tape, manually cut and carefully positioned along the blade chord using digital calipers, as depicted in Figure 2. The collected experimental pressure time history was processed to obtain its Power Density Spectrum (using a 25 Hz bandwidth consistent with simulation analysis), while force/torque data required low-pass filtering to reduce noise.

2.3 Computational domain

To accurately simulate an unbounded acoustic environment, the computational domain was modeled as a large sphere (radius 325 times the propeller diameter) with the propeller at its center. Acoustic sponge layers were applied beyond a radius of 15 propeller diameters to dissipate outgoing sound waves and prevent reflections. The flow was simulated for 10 initial propeller rotations to allow the flow to fully develop, followed by 10 rotations during which aerodynamic and acoustic data were collected. Following previous research indications [5, 6], the tripping structures were applied only on the suction side of the propeller blades. These computationally intensive simulations were executed on the high-performance computing cluster at UFSC.

Figure 2: Experimental tripping device geometry.

2.3.1 Mesh

The overall computational domain is spherical and featured 10 nested refinement levels, creating progressively finer resolution towards the propeller located at the center. To handle the propeller's rotation, a moving mesh technique was employed, involving an inner domain that rotates with the propeller (defined by a Local Reference Frame) connected to a fixed outer domain via an interface.

Special mesh refinement is applied near the propeller blade surface, particularly concentrating on the tips, leading edges, and trailing edges, as these areas are expected to be primary noise sources. This targeted refinement aims to accurately capture viscous effects and the boundary layer development, utilizing approximately 3 million voxels. The mesh design sought to achieve wall y+ values below 5 to resolve the viscous sublayer fully. While some regions exhibit slightly higher y+ values, most of the surface remains below 30, a resolution deemed sufficient for capturing the essential boundary layer physics.

2.3.2 *Numerical Tripping*

The geometry of the boundary layer tripping device used in the simulations is generated based on a characteristic zig-zag pattern, similar to a triangular wave, as depicted in figure 3. The dimensions of this trip are not uniform along the blade, as they adapt and scale based on the local chord length of the airfoil section at different radial positions along the propeller blade.

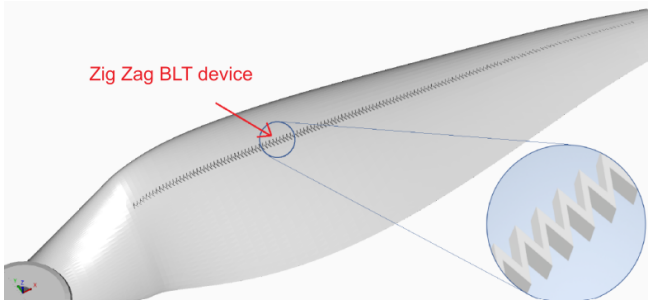

Figure 3: Numerical tripping device geometry.

Specific geometric features define the trip: its position relative to the chord cross section (varied in the calculated natural transition line and from 25% to 75% of the chord), while its amplitude (vertical distance between peaks and valleys) is 3.0% of the local chord. Both the trip's height (protrusion from the surface) and its thickness (dimension in the flow direction) are set at 1.5% of the local chord.

3. RESULTS

Table 1 presents the values and percentual differences of torque values obtained from numerical simulations under various tripping conditions against the baseline experimental untripped case. The main ideia is to verified the changes, relative to the untriped experimental case, for different tripping position numerically. The untripped numerical result shows good agreement with the experimental data, with a relative error of only 3.66%. However, when tripping is introduced and intensified, the numerical torque values progressively diverge from the experimental reference. Notably, the automatic and 0.25C tripping cases exhibit substantial deviations, with relative errors of 21.95% and 32.32%, respectively.

Similarly, Table 2 shows a clear trend of decreasing thrust with increasing tripping, along with rising relative errors. The numerical simulation without tripping again shows the closest match to the experimental thrust, with a 12.76% relative error. The most extreme case, with 25% tripping, reaches a relative error of 19.05%.

Table 1: Comparison of numerical torques and experimental results, with relative errors compared to the untripped Experimental case.

Condition	Torque (N.m)	Relative Error (%)
Without *Tripping* Experimental	0.164	-
Without *Tripping* Numerical	0.170	3.66
Tripping 75% Numerical	0.171	4.27
Tripping 50% Numerical	0.187	14.02
Tripping Automatic Numerical	0.200	21.95
Tripping 25% Numerical	0.217	32.32

Table 2: Comparison of numerical thrusts and experimental results, with relative errors compared to the untripped experimental case.

Condition	Thrust (N)	Relative Error (%)
Without *Tripping* Experimental	8.46	-
Without *Tripping* Numerical	7.38	12.76
Tripping 75% Numerical	7.07	16.43
Tripping 50% Numerical	6.96	17.75
Tripping Automatic Numerical	6.88	18.68
Tripping 25% Numerical	6.85	19.05

Figures 4 reveal the narrow band spectra for all the positiong considered for numerical cases, respectively. The first column representing the -45^o microphone, the second column representing the 0^o microphone, and the third column representing the 45^o microphone position. For the numerical cases, the figures show how the tripping positioned in 0.25C and the automatic tripping positions following the natural transition line present higher and lower levels respectivelly. Those different are more concentrated in the broadband noise levels. Some differents in the BPFs are observed for outer microphone positions (-45^o and 45^o) for the tripping positioned in both 0.25C and the automatic tripping positions.

In Figure 5 the experimental results are presented in a similar manner. These results show more similar trends, but it is important to observe that the levels are lower than the numerical cases, especially for the broadband noise. It is noteworthy that the tripping position at 0.25C still present the higher broadband noise levels, similar to the numerical results.

The numerical and experimental direct comparison is beyond the scope of this work, considering that the

two tripping differ in construction. As pointed out in the methodology, the numerical tripping is a zig-zag tripping with a height of 0.5 mm, while the experimental tripping is a straight trip.

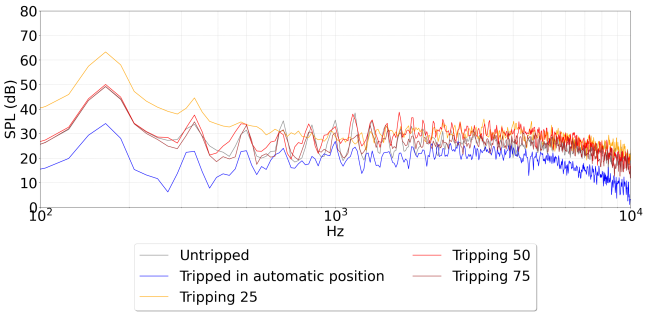

(a) Microphone -45^o

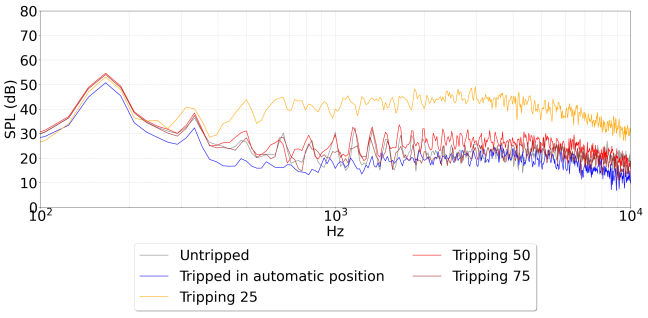

(b) Microphone 0^o

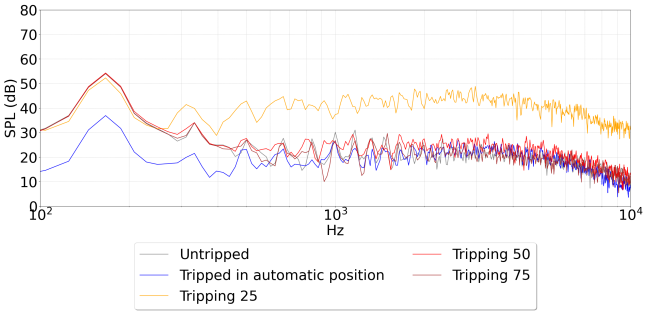

(c) Microphone 0^o

Figure 4: Narrow band spectra for many tripping position for the numerical cases.

A complementary result is presented in Figure 6, which shows the modeled turbulent viscosity, calculated based on the subgrid turbulence model, for the automatic tripping position and the untripped case in the numerical simulation. In the absence of tripping, this variable is consistently higher than in the tripped case. This indicates

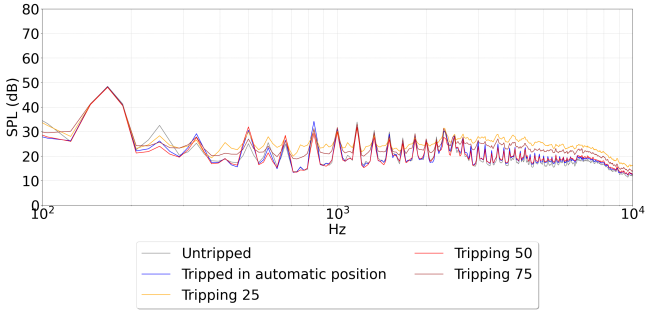

(a) Microphone -45^o

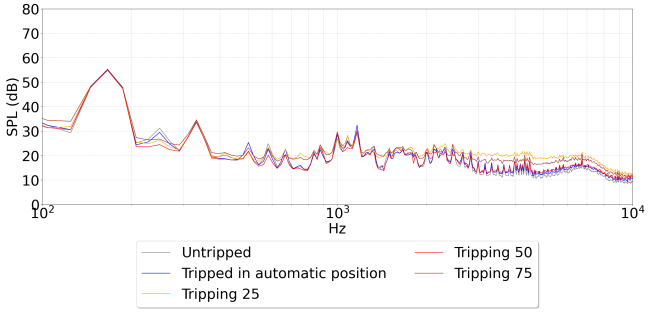

(b) Microphone 0^o

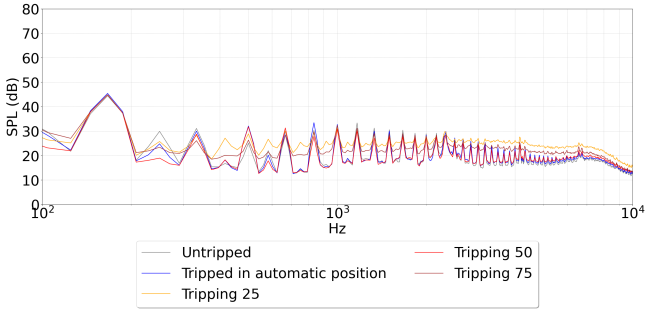

(c) Microphone 45^o

Figure 5: Narrow band spectra for many tripping positions for the experimental cases.

that the tripping is able to force the transition to solved turbulence. A specific analysis of the RANS/LES model transition is beyond the scope of this work.

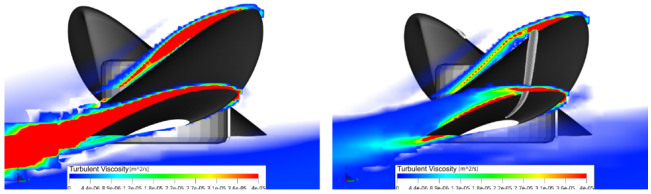

Figure 6: and for the tripping positions.

4. CONCLUSIONS

In this paper, various tripping cases were investigated both numerically and experimentally for aerodynamics and acoustic results, demonstrating important differences due to the positioning of a boundary layer tripping (BLT) device. The BLT device position was varied according to the propeller cross section chord arbitrarily (from 0.25 to 0.75 of the secion chord,c) and using a low-order viscous panel transition model to determine the natural transition line. The results were compared to an untripped case, which served as a baseline for evaluating the impact of tripping on torque, thrust, and the acoustic results are presented for all the cases considered.

From these results, simulations without tripping most closely match the experimental data, showing relatively small errors of 3.66% for torque and 12.76% for thrust. As soon as tripping is introduced, especially in the automatic and 0.25c cases, the discrepancies grow considerably, with torque errors exceeding 30% and thrust errors approaching 20%. Spectral analyses reveal that numerical results for tripped configurations produce higher broadband noise compared to experiments. Additionally, numerical tripping present important differences between tripping cases, with the 0.25c and automatic tripping positions showing the highest and lowest levels, respectively. In contrast, the experimental results show a more consistent trend across all tripping positions, with the 0.25c case still exhibiting the highest broadband noise levels. These differences can be partly attributed to the distinct ways tripping was implemented numerically versus experimentally. In the numerical simulations, zig-zag tripping was used, while the experimental setup employed a straight trip. This discrepancy in design and implementation likely contributed to the observed differences in results. Finally, a closer look at the turbulent viscosity fields indicates that tripping accelerates flow transition, which also influences aerodynamic and aeroacoustic behavior. Overall, these findings underscore the significance of tripping position and design in shaping propeller performance and noise characteristics, highlighting the need for careful consideration in both numerical simulations and experimental setups. In future works, it is expected that simulations will match the experimental tripping design and further improvements in the numerical setup model are expected.

5. REFERENCES

[1] C. A. Lyon, M. S. Selig, and A. P. Broeren, "Boundary layer trips on airfoils at low Reynolds numbers," in *35th Aerospace Sciences Meeting & Exhibit (AIAA)*, (Reno, NV), January 1997.

[2] D. S. Souza, "Simulação numérica de ruído de eslate em configurações práticas usando um código comercial," Dissertação de Mestrado, Escola de Engenharia de São Carlos, Universidade de São Paulo, São Carlos, SP, 2012.

[3] M. Scholz, T. P. Chong, and E. Smith, "The Effect of Tripping Height and Spanwise Homogeneity on the Flow and Noise Characteristics of a NACA-0012 Aerofoil." Conference/Preprint (details not specified), 2022.

[4] D. Systèmes, *PowerFLOW 2022-R3 Documentation*, 2023. Version 2021-R4.

[5] D. Casalino, E. Grande, G. Romani, D. Ragni, and F. Avallone, "Definition of a benchmark for low reynolds number propeller aeroacoustics," *Aerospace Science and Technology*, vol. 113, p. 106707, 2021.

[6] G. Romani, E. Grande, F. Avallone, D. Ragni, and D. Casalino, "Performance and noise prediction of low-reynolds number propellers using the lattice-boltzmann method," *Aerospace Science and Technology*, vol. 125, p. 107086, 2022. SI: DICUAM 2021.

[7] A. Leslie, K. C. Wong, and D. Auld, "Broadband noise reduction on a mini-UAV propeller," in *14th AIAA/CEAS Aeroacoustics Conference (29th AIAA Aeroacoustics Conference)*, 2008. AIAA Paper, 2008.

[8] T. Zhao and et al., "Noise reduction on a low Reynolds number propeller," *Journal of Physics: Conference Series*, vol. 2569, no. 1, p. 012050, 2023.